



Ultraviolet stimulated emission from high-temperature-annealed MgO microcrystals at room temperature

Soma, Haruka

Uenaka, Yuki

Asahara, Akifumi

Suemoto, Tohru

Uchino, Takashi

(Citation)

Applied Physics Letters, 106(4):041116-041116

(Issue Date)

2015-01-26

(Resource Type)

journal article

(Version)

Version of Record

(Rights)

©2015 American Institute of Physics. This article may be downloaded for personal use only. Any other use requires prior permission of the author and the American Institute of Physics. The following article appeared in Journal of Applied Physics 106(4), 041116 and may be found at <http://dx.doi.org/10.1063/1.4907321>

(URL)

<https://hdl.handle.net/20.500.14094/90002685>



Ultraviolet stimulated emission from high-temperature-annealed MgO microcrystals at room temperature

Haruka Soma, Yuki Uenaka, Akifumi Asahara, Tohru Suemoto, and Takashi Uchino

Citation: [Applied Physics Letters](#) **106**, 041116 (2015); doi: 10.1063/1.4907321

View online: <http://dx.doi.org/10.1063/1.4907321>

View Table of Contents: <http://scitation.aip.org/content/aip/journal/apl/106/4?ver=pdfcov>

Published by the [AIP Publishing](#)

Articles you may be interested in

[Stimulated emission from ZnO thin films with high optical gain and low loss](#)

Appl. Phys. Lett. **102**, 171105 (2013); 10.1063/1.4803081

[Stimulated emission at 340 nm from AlGaIn multiple quantum well grown using high temperature AlN buffer technologies on sapphire](#)

Appl. Phys. Lett. **95**, 161904 (2009); 10.1063/1.3253416

[Phonon-assisted stimulated emission from single CdS nanoribbons at room temperature](#)

Appl. Phys. Lett. **88**, 173102 (2006); 10.1063/1.2198089

[Room-temperature stimulated emission of excitons in ZnO/\(Mg,Zn\)O superlattices](#)

Appl. Phys. Lett. **77**, 2204 (2000); 10.1063/1.1315340

[Room-temperature deep-ultraviolet-stimulated emission from Al_xGa_{1-x}N thin films grown on sapphire](#)

Appl. Phys. Lett. **74**, 245 (1999); 10.1063/1.123269



Ultraviolet stimulated emission from high-temperature-annealed MgO microcrystals at room temperature

Haruka Soma,¹ Yuki Uenaka,¹ Akifumi Asahara,² Tohru Suemoto,² and Takashi Uchino^{1,a)}

¹Department of Chemistry, Graduate School of Science, Kobe University, Nada, Kobe 657-8501, Japan

²Institute for Solid State Physics, University of Tokyo, 5-1-5 Kashiwanoha, Kashiwa, Chiba 277-8581, Japan

(Received 2 December 2014; accepted 22 January 2015; published online 30 January 2015)

Research on semiconductor nanowires underlies the development of the miniaturization of laser devices with low cost and low energy consumption. In general, nanowire lasers are made of direct band gap semiconductors, e.g., GaN, ZnO and CdS, and their band-edge emissions are used to achieve optically pumped laser emission. In addition to the existing class of nanowire lasers, we here show that air-annealed micrometer-sized MgO cubic crystals with well-defined facets exhibit room-temperature stimulated emission at 394 nm under pulsed laser pumping at ~ 350 nm. Surface midgap states are assumed to be responsible for the excitation and emission processes. The present findings will not only provide opportunities for the development of miniaturized lasers composed of insulating oxides, but will also open up functionality in various families of cubic crystalline materials. © 2015 AIP Publishing LLC. [<http://dx.doi.org/10.1063/1.4907321>]

Ever since the report of room temperature laser emission from ZnO thin films^{1,2} and nanowires³ under optical pumping, semiconductor nanostructure lasers have attracted intense interest as promising ultracompact and low power consumption photonic lasers.^{4–9} Because of their dislocation free single-crystalline nature and atomically smooth surface, semiconductor nanowires provide both a gain medium and a cavity for lasing. It has also been proposed that the coherent feedback is provided by recurring scattering events in semiconductor nanostructures, leading to random lasing.^{10–13} Note also that in the operation of optically pumped semiconductor lasers, near-band-edge excitonic emissions are normally used and amplified in the respective nanocavities,⁷ allowing tunable emission by changing the bandgap of the semiconductors.¹⁴

In contrast to the case of semiconductors, optically pumped band-edge lasing is difficult to achieve in insulating oxides with large band gap energy E_g (e.g., $E_g \geq 6$ eV) because of the unavailability of the pumping source, even when the nano/microstructures appropriate for lasing are possible to fabricate. It should be noted, however, that some of the insulating oxides, e.g., magnesium oxide (MgO) with $E_g \sim 7.8$ eV, exhibit unusual absorption at much lower energy than the band gap of the corresponding bulk materials because of the presence of defect and/or surface states.^{15–17} This allows us to predict that optically pumped lasers can be realized even in insulating oxides by utilizing these midgap states. Indeed, we have recently reported that broadband laser emission in the near-ultraviolet to the blue-green spectral range is realized in MgO microcrystals with neutral and positively charged oxygen vacancies (F and F^+ centers).^{18–20} In MgO, the F and F^+ color centers absorb essentially the same energy of ~ 5 eV (~ 250 nm) and show different photoluminescence (PL) bands peaking at ~ 500 and ~ 385 nm, respectively.^{21–23} Accordingly, the laser actions is achieved

in these colored MgO crystals under pulsed laser excitation using the fourth harmonic (266 nm) of a pulsed Nd:yttrium-aluminum-garnet (YAG) laser.^{18–20}

In this letter, we further show that the MgO microcrystals exhibit a different but intriguing lasing behavior when the samples are annealed in air atmosphere at temperatures of 1000 °C and above. The thus annealed MgO microcrystals hardly show PL bands related to the F and F^+ centers, but the laser action is still achieved under pulsed laser excitation at longer wavelength or by excitation with the third harmonic (355 nm) of a Nd:YAG laser. The lasing characteristics, including emission wavelength, lasing threshold, width of the laser line, and decay time, are inherently different from those of the MgO-based color center laser reported previously.

The MgO microcrystals used in this work are basically the same with those reported in Ref. 20 except the post-annealing procedure performed in air atmosphere. We hence briefly describe the sample preparation procedure as follows. The Mg/B₂O₃ mixture of molar ratio of 5:1 was put in a cylindrical alumina crucible. This crucible was located inside a larger rectangular alumina crucible, which was closed with a 4-mm-thick alumina lid. This set of crucibles was placed in an electric furnace. The temperature of the furnace was raised to 700 °C at a rate of ~ 10 °C/min and kept constant at 700 °C for 2 h under flowing argon (0.1 l/min) environment. After the heating process, the furnace was naturally cooled to room temperature under argon gas environment. It was found that MgO powders were preferentially deposited outside the inner crucible. We then annealed the samples in the temperature regions from 700 to 1100 °C for 1 h in air atmosphere.

Powder x-ray diffraction (XRD) patterns of the samples were obtained with a diffractometer (Rigaku, SmartLab) using Cu K α radiation. Scanning electron microscopy (SEM) and an energy dispersive X-ray (EDX) spectroscopy were conducted with a scanning electron microscope (JEOL, JSM-5610LVS) with energy dispersive spectrometer. Infrared absorption spectra were measured with a Fourier transform infrared (FTIR)

^{a)}Author to whom correspondence should be addressed: Email: uchino@kobe-u.ac.jp

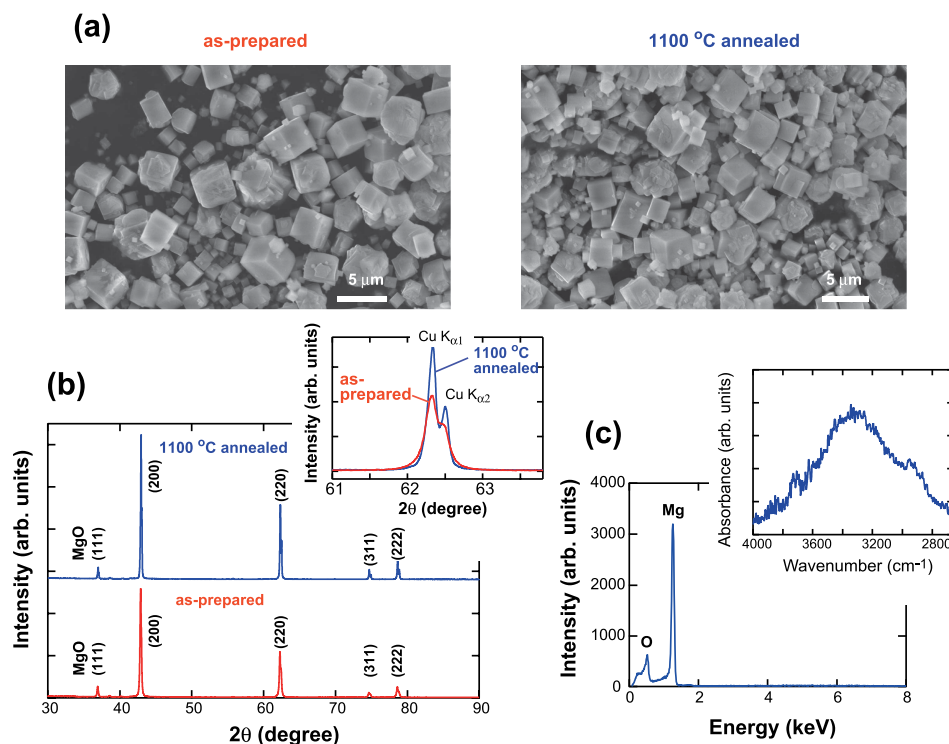


FIG. 1. Structural characterization of the MgO microcrystals. (a) Scanning electron microscopy images and (b) X-ray diffraction patterns of the as-prepared and 1100-°C annealed MgO samples. The inset in (b) shows an enlarged plot of the (220) Bragg peaks. (c) The energy dispersive X-ray spectrum and the FTIR spectrum (inset) of the 1100-°C annealed sample.

spectrometer (Nicolet, iS5) with an attenuated total reflectance (ATR) option. Inductively coupled plasma atomic emission spectrometry (ICP-AES) was performed with an ICP spectrometer (SII, SPS3100) with a maximal power of 1.6 kW. Steady state PL spectra were recorded on a spectrofluorometer (JASCO, FP 6600) by using a monochromated xenon lamp (150 W). For pulsed laser experiments, we used two different laser sources. One is the third-harmonic (355 nm) of a nanosecond Nd: YAG laser (Spectra Physics, INDI 40, pulse width 8 ns, repetition rate 10 Hz). During the experiments using this laser source, the pump beam was irradiated onto the powder in a quartz cell without focusing the laser beam (beam spot size ~ 10 mm), and light emission was collected with a 300 lines/mm grating and a gated image intensifier in combination with a charge-coupled device (CCD) camera. The other laser source is a femtosecond Ti:sapphire laser system with an optical parametric amplifier (OPA). We used the 350-nm pulses generated with OPA (Light Conversion, TOPAS-C), which was seeded by a 1-kHz Ti:Sapphire regenerative amplifier system (Spectra Physics, TSUNAMI 3160C and Spitfire) producing 120-fs pulses at 800 nm. This femtosecond laser system, combined with a streak camera (Hamamatsu Photonics, C5680), was used to obtain time-resolved photoluminescence (TRPL) spectra. The overall time resolution of the measuring system was 14 ps. For the TRPL measurements, the samples were excited by a femtosecond laser pulse focused to a spot size of 100 μm diameter. Time-integrated PL (TIPL) signals were also measured with the same optical arrangement as the TRPL, except that fiber-optic spectrometer was used to monitor the emitted signals. All the PL measurements in this work were carried out at room temperature under ambient atmospheric conditions.

Figure 1 summarizes the results of structural properties obtained for the as-prepared and 1100-°C annealed MgO samples. Scanning electron microscopy (SEM) images and X-ray diffraction (XRD) pattern demonstrate that the as-prepared

sample consists of micrometer-sized MgO cubic crystals. Although there exists a variation in size, most of them have the size of ~ 1 – 3 μm. SEM images shown in Fig. 1(a) also show that the size and apparent morphology of the MgO microcrystals are hardly influenced by air annealing. Note, however, that the XRD peaks become sharper after air annealing [see the inset of Fig. 1(b)], indicating that the air annealing procedure is effective in increasing the crystallinity of the MgO microcrystals. No appreciable contamination was detected in the EDX of the annealed MgO microcrystals [see Fig. 1(c)]. The ICP analysis also confirmed that the level of an undesirable metal impurity such as Zn ions in the annealed MgO microcrystals is below 0.001 ppm.

We then measured the steady state PL spectra of the as-prepared and air-annealed samples. As shown in Fig. 2, as-prepared MgO microcrystals exhibit two broad photoluminescence (PL) emission bands at 385 and 500 nm under

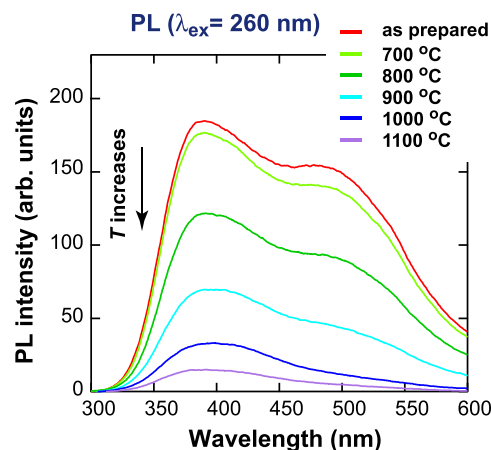


FIG. 2. Steady state photoluminescence spectra of the MgO samples annealed at the designated temperatures. The excitation wavelength is 260 nm.

excitation by photons with energy of 4.8 eV (260 nm) at room temperature. These two PL bands at 385 and 500 nm are attributed to positively charged oxygen vacancies (F^+ centers) and neutral oxygen vacancies (F centers), respectively.^{18–23} Thus, the MgO microcrystals prepared by the current method contain a substantial amount of oxygen vacancies, in agreement with our previous results.^{18–20} We found that the intensity of these two PL bands substantially decreases with increasing annealing temperature up to 1100 °C (see also Fig. 2). Thus, oxygen vacancies are filled by atmospheric oxygen during the air annealing process, resulting in the well-crystallized MgO microcrystals with less defect centers.

We next investigate the results of PL measurements of the as-prepared MgO microcrystals conducted under nanosecond pulsed laser excitation. As mentioned earlier, we have previously reported that the as-prepared samples exhibit color-center-based laser emission under excitation with the fourth harmonic (266 nm) of a Nd:YAG laser.^{18–20} As shown in Fig. 3(a), however, excitation with the third harmonic (355 nm) of a Nd:YAG laser does not induce a lasing action. This is not surprising because the excitation with 355-nm pulse is not effective in inducing the emission of the F^- and F^+ centers. One only sees a gradual development of a broad PL band at ~ 385 nm, with a full width at half maximum (FWHM) of 0.22 eV, with increasing pump fluence. Spectrally integrated emission intensity as a function of pump fluence is shown in Fig. 3(b). The PL intensity tends to saturate with increasing fluence. The saturation behavior is well described by the absorption saturation model²⁴

$$I(J) \propto J/(1 + J/I_s), \quad (1)$$

where $I(J)$ is the emission intensity, J is the pump fluence, and I_s is the parameter related to the saturation intensity. Thus, the present PL saturation behavior can be interpreted in terms of the ground-state depletion under high density excitation.

On the other hand, the air-annealed MgO microcrystals do not show PL saturation but demonstrate a light amplification behavior under pulsed laser pumping. As the pump fluence is increased from ~ 1 to ~ 15 mJ/cm², a broad PL band with a FWHM of 0.11 eV is developed at 394 nm [Fig. 3(c)]. Upon further increase in pump fluence to ~ 20 mJ/cm², the emission band becomes narrow, resulting in a sharp peak with a FWHM of 0.03 eV. Above this threshold, the emission intensity increases rapidly in a linear manner with the pump fluence [see Fig. 3(d)]. The narrow line width and the rapid linear increase in intensity prompts us to assume that laser-like stimulated emission takes place in the well-annealed MgO microcrystals.

To further corroborate the expected laser action in the well-annealed MgO microcrystals, we carried out time-resolved PL measurements with 350 nm femtosecond laser pulses from an OPA pumped by a mode-locked Ti:sapphire regenerative amplifier. As shown in Fig. 4(a), a superlinear increase in PL intensity at ~ 390 nm was also demonstrated although the observed threshold (~ 10 mJ/cm²) is slightly lower than that obtained under nanosecond excitation (~ 20 mJ/cm²). The lower lasing threshold is probably due to the suppression of decay and recombination events under femtosecond pumping.⁶ Figure 4(b) shows the PL decay curves under different pump fluences. For below-threshold pumping (6.5 mJ/cm²), the emission decays on the time scale of sub-nanoseconds [see also the

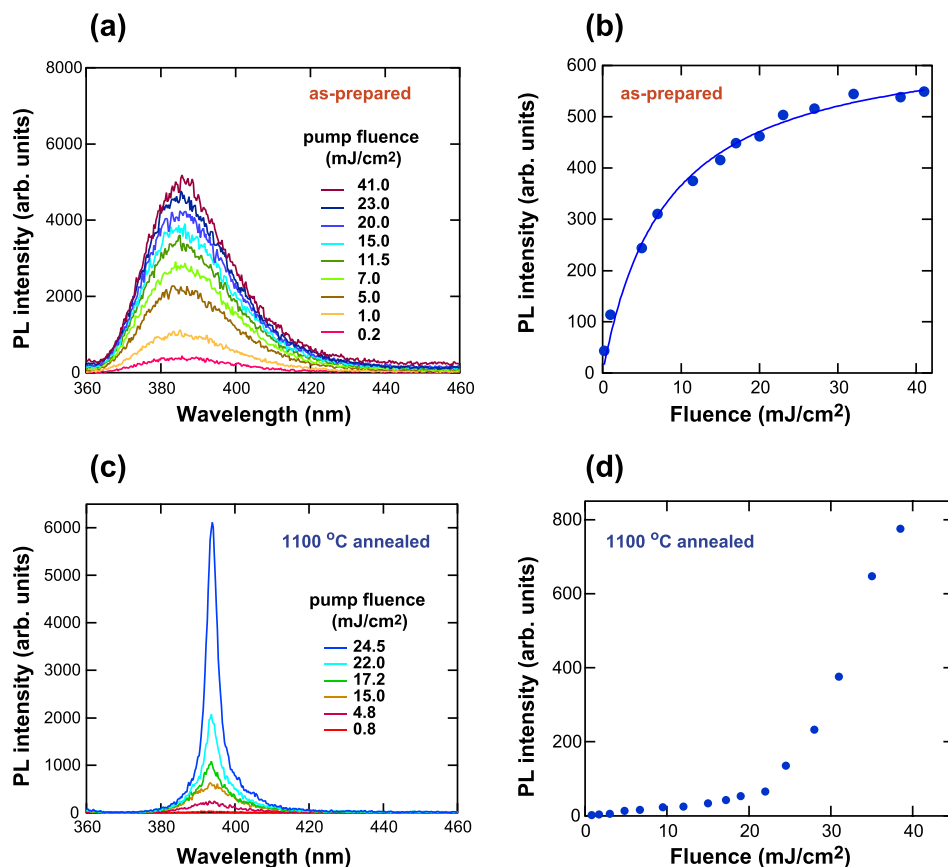


FIG. 3. PL characteristics of (a) and (b) the as-prepared and (c) and (d) the 1100-°C annealed MgO microcrystals obtained under nanosecond pulsed laser excitation. The third harmonic of a nanosecond Nd:YAG laser is used as a pump source. (a) and (c) Laser fluence dependence of the emission spectra. (b) and (d) Spectrally integrated emission intensity as a function of pump fluence. The solid line in (b) shows the best fit of the data with Eq. (1).

streak-camera images in Fig. 4(c)]. For above-threshold pumping (10.4 mJ/cm^2), the transient PL is dominated by a picosecond ($\sim 20 \text{ ps}$) decay process, which includes the time resolution of the present system ($\sim 14 \text{ ps}$), accompanied by narrowing of the emission band, as seen in the streak-camera image shown in Fig. 4(d). These changes in the emission characteristics with pump fluence are consistent with the assumption that stimulated emission, or lasing, is realized in the air-annealed MgO microcrystals.

It should be noted that the lasing characteristics of the air-annealed MgO microcrystals is totally different from that of the as-prepared ones in terms of the excitation and emission wavelengths, the lasing threshold, the spectral width of the laser emission line, and the decay constant, as summarized in Table I. Hence, such lasing properties as observed in the air-annealed MgO microcrystals have not been reported previously. Since the present MgO microcrystals have well-defined facets, it would be safe to assume that the observed coherent feedback is provided by the Fabry-Perot mode of the natural optical cavity derived from the two facing facets of the microcrystals.²⁵ As for the as-prepared samples, however, atomically flat facets will not be expected to exist because of the presence of the oxygen vacancies. This probably explains the reason why the as-prepared MgO microcrystals do not show lasing action [see Fig. 3(a)]. As for nanostructured systems, however, there is also a possibility that lasing occurs via recurrent light scattering in a

three-dimensional random medium, or random lasing.^{10–13} It is presently unclear which mechanism is indeed responsible for the lasing behavior of the air-annealed MgO crystals. Further measurements using single MgO microcrystals will be required to make clear the origin of the feedback mechanism.

Finally, we discuss a possible origin of the emission states responsible for the $\sim 390\text{-nm}$ PL band under pulsed laser excitation at $\sim 350 \text{ nm}$. Considering that MgO often exhibit the PL emission in this spectral region under excitation with photons of $\sim 350 \text{ nm}$,¹⁷ we suggest that the $\sim 390\text{-nm}$ PL band is ascribed to OH-related emission centers at the surface of MgO. Since the present PL measurements were carried out under ambient atmospheric conditions, it is most likely that chemically active edge and corner sites of MgO are covered with hydroxyl Mg-OH groups.^{26–28} We indeed confirmed from Fourier transform infrared (FTIR) spectroscopic studies that the $1100\text{-}^\circ\text{C}$ annealed sample exhibits a broad absorption band in the O-H stretching frequency region^{28,29} ($3800\text{--}2800 \text{ cm}^{-1}$) [see the inset of Fig. 1(c)]. It has been reported that OH groups at oxide surfaces are characterized by a PL decay time of a few nanosecond or less, when measured under ambient conditions.³⁰ This is in accordance with the decay characteristics observed under below-threshold pumping [see Fig. 4(b)]. As compared with the surface atoms at the edge and corner sites, those at the (100) flat surfaces are, in general, rather stable against hydration.^{17,27,28} It is hence probable that the amount of the

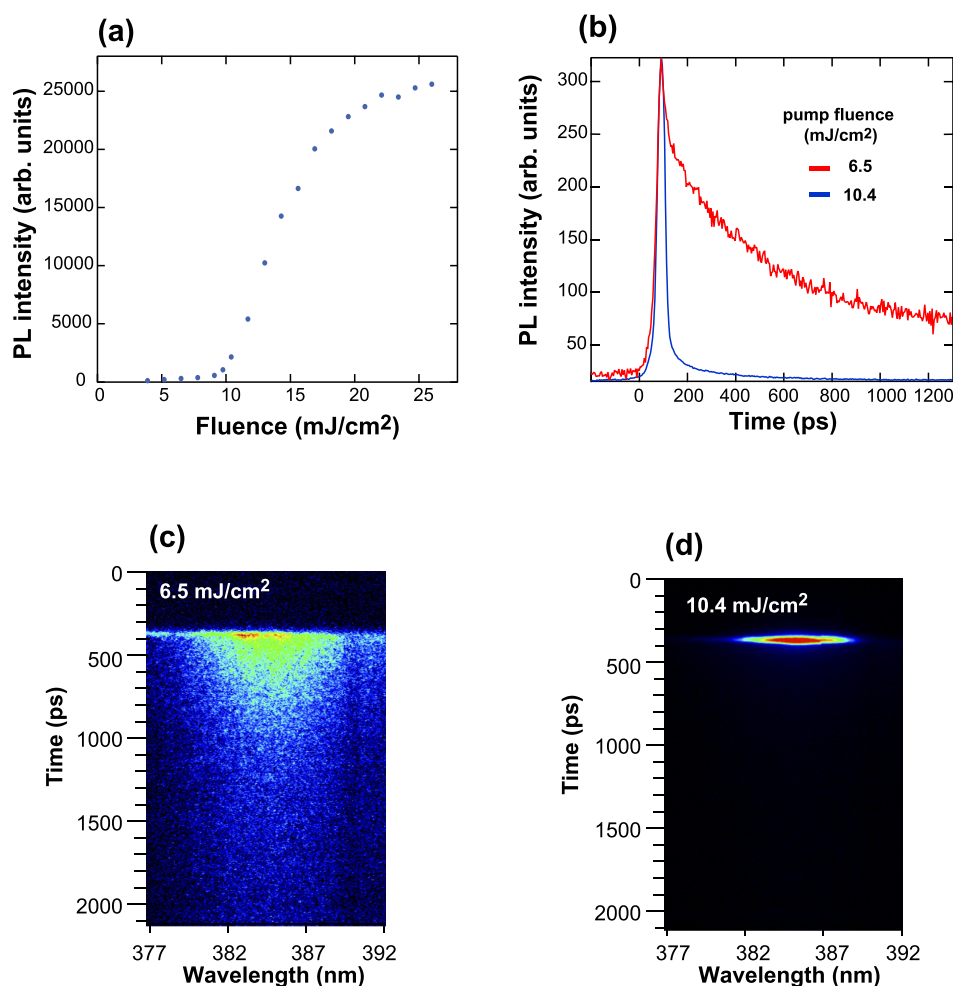


FIG. 4. PL characteristics of the $1100\text{-}^\circ\text{C}$ annealed MgO microcrystals obtained under femtosecond pulsed laser excitation at 350 nm . Femtosecond laser pulses at 350 nm were generated with an OPA pumped by a Ti:sapphire-regenerative amplifier. (a) Emission peak ($\sim 390 \text{ nm}$) intensity as a function of pump fluence. (b) Normalized decay profiles of the emission recorded at different pump fluences. (c) and (d) Streak-camera images obtained under the designated pump fluences.

TABLE I. Lasing characteristics (excitation wavelength λ_{ex} , emission wavelength λ_{em} , lasing threshold E_{th} , width of the laser line ΔE , and decay time τ) for the air-annealed MgO microcrystals and the comparison with those of the as-prepared ones reported previously.^{18–20}

sample	λ_{ex} (nm)	λ_{em} (nm)	E_{th} (mJ/cm ²)	ΔE (meV)	τ (ns)
air-annealed	~350	394	20	0.03	≤0.02
as-prepared	~260	384	~100	~0.1	20

surface-related OH groups in the present MgO microcrystals is rather low. This probably accounts for the fact that as for the 1100-°C annealed samples, the ultraviolet (UV) PL band is observed only at excitation levels higher than ~1 mJ/cm² [see Fig. 3(a)]. At sufficiently high excitation levels (≥ 20 mJ/cm²), the population inversion will be achieved between a certain emission state and the ground state, eventually resulting in the laser emission. It has been demonstrated that some Mg-OH groups are still present at the surface of MgO even after outgassing at temperatures up to ~1000 K.^{28,31} Thus, we believe that the expected OH groups remain at least partly intact even at high laser pumping intensities and are hence responsible for the laser emission. It should be mentioned, however, that the present samples show no PL emission even under pulsed laser excitation when annealed under O₂ atmosphere.²⁵ This observation suggests a possibility that certain unidentified surface defects can contribute to the generation of the UV PL band. We should also note that the lasing action of the MgO microcrystals remains stable for more than six months when the samples are stored in a desiccator filled with silica gel desiccants. This ensures the robustness of the present MgO microcrystals in terms of the laser action.

In conclusion, our SEM and XRD data show that well-crystallized MgO microcrystals with the size of ~1–3 μm are prepared by solid phase reaction between Mg and B₂O₃ under Ar atmosphere, combined with post annealing in air. Room-temperature lasing action at 394 nm was demonstrated from the well-annealed MgO microcrystals under pulsed laser excitation with wavelength of ~350 nm. Surface emission centers associated with hydroxylated species at the edges and corners of the microcrystals are expected to be responsible for the 394-nm laser emission. The natural optical cavity derived from the facets of the microcrystals or recurrent light scattering among the microcrystals is responsible for the coherent feedback. It should also be noted that the observed lasing threshold under ~10 ns pulsed laser excitation is ~20 mJ/cm² per pulse (or ~200 kW/cm²), which is comparable to the typical values of lasing threshold observed for semiconductor nanowire lasers under similar excitation conditions.^{2,4,8} The present observation will hence provide a solid-state system that allows light amplification by changing the scale and surface states of otherwise optically inert insulating oxides.

A part of this work was carried out by the Joint research in the Institute for Solid State Physics, the University of Tokyo.

- ¹P. Zu, Z. K. Tang, G. K. L. Wong, M. Kawasaki, A. Ohtomo, H. Koinuma, and Y. Segawa, *Solid State Commun.* **103**, 459 (1997).
- ²D. M. Bagnall, Y. F. Chen, Z. Zhu, T. Yao, S. Koyama, M. Y. Shen, and T. Goto, *Appl. Phys. Lett.* **70**, 2230 (1997).
- ³M. H. Huang, S. Mao, H. Feick, H. Yan, Y. Wu, H. Kind, E. Weber, R. Russo, and P. Yang, *Science* **292**, 1897 (2001).
- ⁴J. C. Johnson, H. Yan, R. D. Schaller, L. H. Haber, R. J. Saykally, and P. Yang, *J. Phys. Chem. B* **105**, 11387 (2001).
- ⁵J. C. Johnson, H. J. Choi, P. Knutsen, R. D. Schaller, P. Yang, and R. J. Saykally, *Nat. Mater.* **1**, 106 (2002).
- ⁶D. J. Sirbulu, M. Law, H. Yan, and P. Yang, *J. Phys. Chem. B* **109**, 15190 (2005).
- ⁷R. Yan, D. Gargas, and P. Yang, *Nat. Photonics* **3**, 569 (2009).
- ⁸M. A. Zimmiller, F. Capasso, S. Müller, and C. Ronning, *Semicond. Sci. Technol.* **25**, 024001 (2010).
- ⁹D. Vanmaekelbergh and L. K. van Vugt, *Nanoscale* **3**, 2783 (2011).
- ¹⁰H. Cao, Y. G. Zhao, S. T. Ho, E. W. Seelig, Q. H. Wang, and R. P. H. Chang, *Phys. Rev. Lett.* **82**, 2278 (1999).
- ¹¹H. Cao, J. Y. Xu, D. Z. Zhang, S.-H. Chang, S. T. Ho, E. W. Seelig, X. Liu, and R. P. H. Chang, *Phys. Rev. Lett.* **84**, 5584 (2000).
- ¹²H. Cao, J. Y. Xu, E. W. Seelig, and R. P. Chang, *Appl. Phys. Lett.* **76**, 2997 (2000).
- ¹³D. S. Wiersma, *Nat. Phys.* **4**, 359 (2008).
- ¹⁴T. Kuykendall, P. Ulrich, S. Aloni, and P. Yang, *Nat. Mater.* **6**, 951 (2007).
- ¹⁵J. D. Levine and P. Mark, *Phys. Rev. Lett.* **144**, 751 (1966).
- ¹⁶A. L. Shluger, P. V. Sushko, and L. N. Kantorovich, *Phys. Rev. B* **59**, 2417 (1999).
- ¹⁷M.-L. Bailly, G. Costentin, H. Lauron-Pernot, J. M. Krafft, and M. Che, *J. Phys. Chem. B* **109**, 2404 (2005).
- ¹⁸T. Uchino and D. Okutsu, *Phys. Rev. Lett.* **101**, 117401 (2008).
- ¹⁹T. Uchino, D. Okutsu, R. Katayama, and S. Sawai, *Phys. Rev. B* **79**, 165107 (2009).
- ²⁰Y. Uenaka and T. Uchino, *Phys. Rev. B* **83**, 195108 (2011).
- ²¹Y. Chen, J. L. Kolopus, and W. A. Sibley, *Phys. Rev.* **186**, 865 (1969).
- ²²L. A. Kappers, R. L. Kroes, and E. B. Hensley, *Phys. Rev. B* **1**, 4151 (1970).
- ²³G. H. Rosenblatt, M. W. Rowe, G. P. Williams, R. T. Williams, and Y. Chen, *Phys. Rev. B* **39**, 10309 (1989).
- ²⁴J. Heber, C. Mühlh, W. Triebel, N. Danz, R. Thielsch, and N. Kaiser, *Appl. Phys. A* **75**, 637 (2002).
- ²⁵See supplementary material at <http://dx.doi.org/10.1063/1.4907321> for a SEM image and a PL spectrum of the O₂-annealed sample. We found that the micrometer-sized MgO cubic crystals tend to aggregate to grow into larger secondary particles when the air-annealed samples are further annealed in O₂ atmosphere at 1000 °C for 2 h. These secondary particles do not have well-defined facets and shapes, in contrast to the original air-annealed MgO microcrystals. In addition, the O₂-annealed samples exhibit no PL emission and hence, no laser action in the UV/visible spectral region under pulsed laser excitation at 355 nm. These results also imply that the well-defined facets of the respective micrometer-sized MgO cubic crystals are, directly or indirectly, responsible for the generation of the UV PL emission and the related laser emission.
- ²⁶S. Coluccia, L. Marchese, S. Lavagnino, and M. Anpo, *Spectrochim. Acta* **43A**, 1573 (1987).
- ²⁷M. Müller, S. Stankic, O. Diwald, E. Knözinger, P. V. Sushko, P. E. Trevisanotto, and A. L. Shluger, *J. Am. Chem. Soc.* **129**, 12491 (2007).
- ²⁸C. Chizallet, G. Costentin, M. Che, F. Delbecq, and P. Sautet, *J. Am. Chem. Soc.* **129**, 6442 (2007).
- ²⁹E. Knözinger, K. H. Jacob, S. Singh, and P. Hofmann, *Surf. Sci.* **290**, 388 (1993).
- ³⁰M. Rückschloss, Th. Wirschem, H. Tamura, G. Ruhl, J. Oswald, and S. Vepřek, *J. Lumin.* **63**, 279 (1995).
- ³¹C. Chizallet, G. Costentin, H. Lauron-Pernot, J.-M. Krafft, M. Che, F. Delbecq, and P. Sautet, *J. Phys. Chem. C* **112**, 19710 (2008).